2.3 Tomographic X-ray projection data

In tomographic X-ray imaging one takes X-ray projection images of an object from several different directions and attempts to recover the inner structure of the object from the data.

We show how such a measurement can be written in the form $\mathbf{m} = A\mathbf{f} + \varepsilon$ and illustrate numerically how the naïve reconstruction approach (1.4) fails.

2.3.1 A simple example: Probing two aluminum slabs

Let us first demonstrate the exponential attenuation law of X-rays using a very simple example, where two aluminum slabs are probed as shown in Figure 2.12. Typically, X-rays emanate from a roughly point-like location inside an X-ray tube. That point is called the *X-ray source* and shown as a black dot in Figures 2.12 and 2.13. Three X-rays are sent traveling towards a detector, each consisting initially of 1000 photons. The detector is capable of counting how many photons arrive at each point. One of the rays arrives at the detector through empty space, delivering all 1000 photons. Another ray travels through an aluminum slab whose width is chosen to be the *half-thickness* of the X-radiation used here. This means that half of the photons entering the slab will be absorbed inside the slab. The third ray encounters two such aluminum slabs. We call these three X-rays the empty-space ray, the one-slab ray, and the two-slab ray, respectively.

The photon count data can now be transformed into line integral data via two simple steps. First, take the logarithm of each photon count. Then, realizing that the integral of the empty-space ray must be zero, subtract each logarithm from the logarithm corresponding to the empty-space ray. As seen from the actual numbers shown in Figure 2.12, the resulting attenuation data is zero for the empty-space ray, a positive number (0.693) for the one-slab ray, and twice that number (1.386) for the two-slab ray.

We have described the basic calibration process for ideal photon count data based on the exponential attenuation law. However, we ignored at least a couple of properties of real-world measurements. First, practical detectors (for instance, charge-coupled devices or CCDs do not provide the actual photon count but rather an integer that is proportional to the photon count. However, this is not a serious problem, as you can find out in Exercise 2.3.2 below. Second, the photon count is not a deterministic number; it is better modeled as a random variable with Poisson distribution. This results in random measurement noise in the data; we will discuss this below.

Figure 2.12. Simple experiment illustrating the attenuation of X-rays and interpretation of measurements. The three black dots show the positions of the X-ray source, and the horizontal lines depict X-rays. The gray boxes are slabs of attenuating material, and their width has been chosen to be the half-thickness of the X-radiation. The vertical thick line is the detector counting how many photons arrive at each point.

2.3.2 From photon count data to line integral data

The two-slab example in Section 2.3.1 is quite simple as it concerns only homogeneous material. Consider now an X-ray traveling through a phantom[1] representing a two-dimensional cross-section of a patient's head along a straight line, as shown in the left panel of Figure 2.13. We place the target slice inside the unit square defined by $0 \le x_1 \le 1$ and $0 \le x_2 \le 1$. For the sake of argument, assume that the X-ray travels along the horizontal path defined by $0 \le x_1 \le 1$ and $x_2 = \frac{1}{2}$.

Interaction between radiation and matter lowers the intensity of the ray. We think of the X-ray having initial intensity $I_0 := I(0)$ when entering the patient's head and smaller intensity $I_1 := I(1)$ when exiting. Also, we denote by $I(x_1)$ the intensity of the X-ray at the point $(x_1, \frac{1}{2})$ while traveling from the source to the detector.

In contrast to the simple homogeneous slab example above, the cross-section of a head contains various tissues with different X-ray attenuation properties. We model this situation using a nonnegative attenuation coefficient function $f(x_1, x_2)$, whose value gives the relative intensity loss of the X-ray within a small distance dx:

$$\frac{dI(x_1)}{I(x_1)} = -f\left(x_1, \frac{1}{2}\right) dx_1.$$

For example, bone has higher attenuation coefficient than brain tissue, and cerebrospinal fluid (white ovals in the left panel of Figure 2.13) provides practically zero attenuation. See the right panel in Figure 2.13 for a plot of the profile $f(x_1, \frac{1}{2})$.

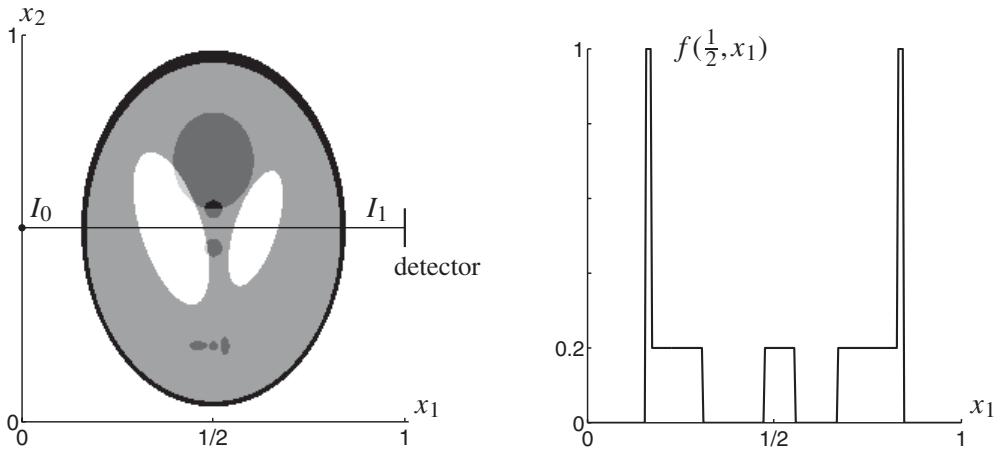

Figure 2.13. X-ray measurement. Left: an X-ray traveling through a simulated cross-section of a human head (a low-contrast version of the infamous Shepp–Logan phantom). Note that high attenuation is shown here as darker shades of gray and low attenuation as lighter shades. Right: plot of the attenuation coefficient along the path of the X-ray.

[1] A *phantom* can be either a physical calibration device or a mathematical model. Here it is a mathematical model to simulate an idealized cross-section of a human head. The use of "phantom" will be clear from the context.

Integration along the X-ray from source to detector gives

$$\int_0^1 f\left(x_1, \frac{1}{2}\right) dx_1 = -\int_0^1 \frac{I'(x_1)}{I(x_1)} dx_1 = \log I_0 - \log I_1. \tag{2.38}$$

Now the right-hand side of (2.38) is known: I_0 by calibration and I_1 from the measurement. The left-hand side of (2.38) consists of an integral of the unknown function f over a straight line, as wished.

Regarding noise, the quantity I_1 is a constant multiple of a Poisson-distributed random variable. It is typically sampled in practice using an analog-to-digital converter that produces integer output containing truncation errors and additional electronic noise. Taking logarithm of I_1 leads to a random variable with remarkably complicated statistics. However, it is usually quite plausible to model the measurement as

$$\log I_0 - \log I_1 = \int_0^1 f\left(x_1, \frac{1}{2}\right) dx_1 + \varepsilon, \tag{2.39}$$

where $\varepsilon \sim \mathcal{N}(0, \sigma^2)$ is a normally distributed random variable. The standard deviation σ of the noise can be estimated, for example, by measuring the same target repeatedly and calculating the standard deviation of the samples. This procedure is a reasonably accurate model when the photon count is large enough; see [414, Appendix].

We remark that in the above model we neglect the energy dependence of the attenuation function. Namely, most X-ray sources produce a multispectral beam, and an energy-dependent f may result in different measured line integrals depending on the propagation direction of the X-ray along the line. This is called *beam hardening*.

2.3.3 Continuous tomographic data: The Radon transform

In the previous section we described how to turn attenuation data from one single X-ray into line integral data concerning a nonnegative, compactly supported attenuation coefficient $f : \mathbb{R}^2 \to \mathbb{R}$. The aim of tomographic imaging is to collect information about f using different angles of view.

Let us define the *Radon transform*, denoted by $\Re$, as follows. We interpret $\theta \in \mathbb{R}$ as an angle measured in radians, and denote by

$$\vec{\theta} := \begin{bmatrix} \cos\theta \\ \sin\theta \end{bmatrix} \in \mathbb{R}^2$$

the unit vector with angle θ with respect to the x_1-axis. The Radon transform of the function f depends on the angular parameter θ and on a linear parameter $s \in \mathbb{R}$ in the following way:

$$\Re f(s, \theta) = \int_{x \cdot \vec{\theta} = s} f(x) dx^{\perp}, \tag{2.40}$$

where $dx^{\perp}$ denotes the one-dimensional Lebesgue measure along the line defined by $\{x \in \mathbb{R}^2 : x \cdot \vec{\theta} = s\}$. We remark that the parametrization of tomographic data provided by formula (2.40) is related to the so-called parallel-beam geometry used in the first-generation computed tomography (CT) scanners in the 1970s.

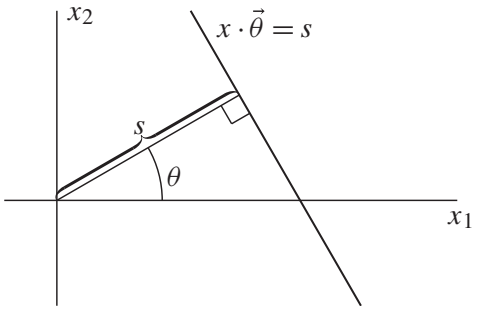

$$\Re f(s,\theta) = \int_{x\cdot\vec{\theta}=s} f(x)dx^{\perp}$$

Figure 2.14. Illustration of the definition (2.40) of the Radon transform. The line $\{x \in \mathbb{R}^2 : x \cdot \vec{\theta} = s\}$ is drawn with a thick line.

Many variations in the data geometry are possible, such as limited angle data, local tomography data, exterior tomography, and combinations thereof. We refer the reader to the classical texts by Natterer [353] and Kak and Slaney [249]. See [353] for analytic inversion formulas, a thorough analysis of the mapping properties of $\Re$, and its generalizations to higher dimensions. See [354] for another perspective on image reconstruction.

The Fourier transform and Radon transform are connected in a simple way. This result is known as the central slice theorem. First, define the Fourier transform in one dimension as follows. See Figure 2.14 for an illustration.

Definition 2.3.1. *The* Fourier transform *of a function defined on* $\mathbb{R}$ *is given by*

$$\mathcal{F}(x)(\xi) = \widehat{f}(\xi) = \frac{1}{(2\pi)^n}\int_{\mathbb{R}} f(x)e^{-ix\xi}dx.$$

Theorem 2.1. *Let f be an absolutely integrable function defined on the whole real line. For any real number r and unit vector $\vec{\theta}$, we have the identity*

$$\int_{-\infty}^{\infty} \Re f(s,\vec{\theta})e^{-isr}ds = \hat{f}(r\vec{\theta}). \tag{2.41}$$

It will prove convenient to have a notation for the one-dimensional Fourier transform of a function in the scalar parameter as appears in the central slice theorem. Let $\tilde{h}(s,\vec{\theta})$ denote such a Fourier transform:

$$\tilde{h}(s,\vec{\theta}) = \int_{-\infty}^{\infty} h(t,\vec{\theta})e^{-its}dt. \tag{2.42}$$

Then the central slice theorem says

$$\widetilde{\Re f}(r,\vec{\theta}) = \hat{f}(r\vec{\theta}).$$

The Radon inversion formula provides a way to obtain f from its Radon transform in the ideal case.

Theorem 2.2. *If f is an absolutely integrable function defined on the real line and $\hat{f}$ is absolutely integrable, then*

$$f(x) = \frac{1}{(2\pi)^2} \int_0^{\pi} \int_{-\infty}^{\infty} e^{isx\cdot\vec{\theta}} \widetilde{\Re f}(s,\vec{\theta})|s|dsd\theta. \tag{2.43}$$

To summarize, this results in the following idealized reconstruction algorithm for X-ray CT imaging:

- Let f be the attenuation coefficient of a two-dimensional slice of a three-dimensional object. Then the intensity $I_{(s,\vec{\theta})}$ of the beam satisfies the differential equation

$$\frac{dI_{(s,\vec{\theta})}}{I_{(s,\vec{\theta})}} = -f(s,\vec{\theta})ds.$$

- We measure the Radon transform of f,

$$\Re f(s,\vec{\theta}) = \log\left(\frac{I_0}{I_d}\right),$$

  where I_0 is the intensity of the beam at the source, and I_d is the intensity of the beam at the detector.

- Reconstruct f from the Radon inversion formula (2.43).

For the filtered back-projection algorithm, we regard the radial integral in the Radon Inversion Formula as a filter. We denote the output of the filter by $\mathcal{G}\Re f(t,\vec{\theta})$, where

$$\mathcal{G}\Re f(t,\vec{\theta}) = \frac{1}{2\pi}\int_{-\infty}^{\infty} \widetilde{\Re f}(r,\vec{\theta})e^{irt}|r|dr.$$

Then, with $t = x\cdot\vec{\theta}$,

$$f(x) = \frac{1}{2\pi}\int_0^{\pi} \mathcal{G}\Re f(x\cdot\vec{\theta},\vec{\theta})d\theta.$$

Note that one sees from this formula that low-frequency components are suppressed by $|r|$ and high-frequency components are amplified. Let's look at the filter a little more carefully. Recall that the Fourier transform of $g'(t)$ is

$$\mathcal{F}(\partial_t g)(\xi) = i\xi\hat{g}(\xi).$$

Thus if we had r instead of $|r|$ in the Radon inversion formula, we would have had the

$$\text{“inversion formula”} = \frac{1}{2\pi i}\int_0^{\pi} \partial_r \Re f(r,\theta)d\theta.$$

If f is real-valued, this quantity is purely imaginary! Thus, the $|r|$ is very important!

The MATLAB function `iradon.m` in the Image Processing Toolbox implements filtered back-projection. In the subsequent sections, we will be comparing the results of filtered back-projection implemented with `iradon.m` to other inversion techniques.